MITSUBISHI ELECTRIC RESEARCH LABORATORIES
https://www.merl.com

Sparsity-driven Joint Blind Deconvolution-demodulation with Application to Motor Fault Detection

Kelkar, Varun A.; Liu, Dehong; Inoue, Hiroshi; Kanemaru, Makoto

TR2023-026 May 06, 2023

Abstract

Motor current signature analysis (MCSA) has been widely used in motor fault diagnosis by extracting characteristic frequency components in the spectrum of the stator current. However, fault signatures in the motor current are generally weak and easily influenced by noise and spectrum distortion caused by varying loads, especially in the early stage of motor faults. In this paper, we develop a sparsity- driven joint blind deconvolution-demodulation approach to extract small fault signatures of motors operating at a varying load. Results on experimental data demonstrate that our approach can effectively extract fault signatures from real noisy measurements of different load variation patterns.

IEEE International Conference on Acoustics, Speech, and Signal Processing (ICASSP) 2023

Mitsubishi Electric Research Laboratories, Inc.
201 Broadway, Cambridge, Massachusetts 02139

SPARSITY-DRIVEN JOINT BLIND DECONVOLUTION-DEMODULATION WITH APPLICATION TO MOTOR FAULT DETECTION

Varun A. Kelkar[1]*, Dehong Liu*[2]*, Hiroshi Inoue*[3]*, Makoto Kanemaru*[3]

[1] University of Illinois at Urbana-Champaign, IL - 61801, USA
[2] Mitsubishi Electric Research Labs, Cambridge, MA, USA
[3] Mitsubishi Electric Corporation, Amagasaki, Japan

ABSTRACT

Motor current signature analysis (MCSA) has been widely used in motor fault diagnosis by extracting characteristic frequency components in the spectrum of the stator current. However, fault signatures in the motor current are generally weak and easily influenced by noise and spectrum distortion caused by varying loads, especially in the early stage of motor faults. In this paper, we develop a sparsity-driven joint blind deconvolution-demodulation approach to extract small fault signatures of motors operating at a varying load. Results on experimental data demonstrate that our approach can effectively extract fault signatures from real noisy measurements of different load variation patterns.

***Index Terms*—** Blind deconvolution, sparse signal, small signal extraction, motor fault

1. INTRODUCTION

Motor faults such as bearing fault, eccentricity fault, and broken-bar fault, *etc.*, cause asymmetric rotating flux in the air gap between the stator and the rotor, and consequently induce extra frequency components in the stator current. Therefore, when there exists a motor fault, the frequency spectrum of the motor current includes not only the operating frequency component, but also the fault signature frequency component. Depending on the fault type, different faults exhibit different signatures. For instance, for eccentricity fault, the frequency components can be expressed as $f_s \pm mf_r$, where f_s is the frequency of the power supply, f_r is a rotor frequency related to the rotational speed, and $m = 0, 1, 2, ...$ [1].

Motor current signature analysis (MCSA), which aims to extract fault signatures in the frequency domain, has been widely used in motor fault detection. In the past decades, various MCSA-based methods have been developed to detection different types of faults in motors[2, 3, 4, 5]. MCSA-based methods work well in general for motors operating at steady status with a constant load and a constant rotating speed.

However, when the motor under test is operating at varying conditions such as a fluctuating load, the motor current magnitude will vary adaptively to provide enough torque to drive the load. In such a situation, the fault signature, whose magnitude is generally much smaller than the operating frequency component, may be corrupted by the distorted frequency spectrum of the motor current due to varying operations or submerged by noise and other systematic perturbations. This issue becomes more evident when the fault is developing at its early stage. Therefore, it is desirable to develop advanced methods to recover the fault signature from varying motor current [4, 6, 7]. Recent studies have considered specific models of load variations, such as phase modulation due to a sinusoidally varying load [8, 9]. For conditions when the load is varying with a specific pattern, time-frequency analysis methods may be used by analyzing multiple time-domain segments[4, 10]. However, time-frequency analysis methods suffer from an inherent tradeoff between time and frequency resolution [4]. Recently, minimum variance (MV) beamforming-based denoising approach is introduced in this motor fault detection area to extract small fault signature under varying load conditions[11, 12]. MV beamforming-based denoising is good at removing random noise, but not capable of removing structured load fluctuations.

In this work, we propose a sparsity-driven method to extract small-magnitude fault signatures from a distorted time-domain stator current signal of a motor under varying load operations by solving a joint blind deconvolution and demodulation problem. The main contribution of our paper lies in the following three aspects. First, we build a physical model of the stator current by simplifying a set of differential equations that relate the stator current to the operating condition in a complicated, nonlinear way. Second, we cast the problem of recovering the steady-state stator signal with fault signatures as a joint deconvolution-demodulation problem with proper assumptions. Third, we develop a proximal alternating linearized minimization-type method to solve the problem, assuming that the spectrum of the sought-after signal is sparse. We demonstrate the utility of our approach on signals collected from a real two-pole induction motor under varying load conditions.

The manuscript is organized as follows. Sec. 2 describes our physical model of the stator current under slowly varying loads. In Sec. 3 we formulate the fault signal extraction problem as a constrained optimization problem, and propose an approach to solving it. Results on experimental data are provided in Sec. 4, with conclusion drawn in Sec. 5.

2. MODEL OF MOTOR STATOR CURRENT

2.1. Physical model

Without loss of generality, we consider a three-phase motor operating at an open-loop condition, driving a slowly varying load. For time $t \in \mathbb{R}$, let $i_s(t)$ and $i_r(t)$ be the time-domain stator and rotor currents respectively, and $u_s(t)$ and $u_r(t)$ denote the stator and the rotor voltages respectively, all in the space vector representation [13, 14]. The relationships between i_s, i_r, u_s, and u_r is given by [14]:

$$\mathbf{u} = \mathbf{Z}\mathbf{i} + \mathbf{L}\frac{\mathrm{d}\mathbf{i}}{\mathrm{d}t}, \tag{1}$$

This work was finished when Varun A. Kelkar was an intern at MERL.

where $\mathbf{i}(t) = [i_s(t) \;\; i_r(t)]^\top$, $\mathbf{u}(t) = [u_s(t) \;\; u_r(t)]^\top$, and $\mathbf{Z} = \begin{bmatrix} R_s & 0 \\ -j\Omega M & R_r - j\Omega L_r \end{bmatrix}$ and $\mathbf{L} = \begin{bmatrix} L_s & M \\ M & L_r \end{bmatrix}$ are impedance and inductance matrices respectively with parameters defined as follows. R_s and R_r represent stator and rotor resistance respectively, L_s, L_r, and M denote the stator, rotor, and mutual inductance respectively, and Ω is the mechanical angular velocity of the rotor. In the frequency domain, motor currents can be formulated according to (1) as

$$\begin{bmatrix} I_s(\omega) \\ I_r(\omega) \end{bmatrix} = (\mathbf{Z} + j\omega\mathbf{L})^{-1} \begin{bmatrix} U_s(\omega) \\ U_r(\omega) \end{bmatrix}, \tag{2}$$

where $\omega = 2\pi f$ is the angular frequency. Therefore, the transfer function corresponding to the stator and rotor currents can be expressed in the frequency domain as

$$H(\omega) \triangleq \frac{I_s(\omega)}{I_r(\omega)} = \frac{a + jb\omega}{c + jd\omega}, \tag{3}$$

where a, b, c, and d are complex numbers related to the motor parameters and its rotational angular speed Ω. When the motor is operating at a steady state, meaning the angular speed Ω is a constant, $H(\omega)$ is characterized by motor parameters, which could be different for different motors. When the motor is operating at a varying speed or a transient state, $H(\omega)$ is also related to the rotational speed Ω.

On the other hand, since the load is varying slowly, we assume that the motor can track the load change and provide enough electromagnetic torque to drive the load. Let $\tau(t)$ be the electromagnetic torque as a function of time, $i_{ss}(t)$ be the steady-state stator current under constant load in noiseless conditions.The electromagnetic torque can be approximated by the stator current and the rotor current using space vectors as [14]

$$\tau(t) = \kappa i_s(t)^* i_r(t) \approx \kappa i_{ss}(t)^* i_r(t), \tag{4}$$

where κ is a proportionality constant, the superscript $*$ represents the hermitian transpose. This implies

$$i_r(t) = \frac{\tau(t)}{\kappa \|i_{ss}(t)\|^2} i_{ss}(t) \triangleq m(t)x(t), \tag{5}$$

where $m(t) \triangleq \frac{\tau(t)}{\kappa \|i_{ss}(t)\|^2}$ is a modulation signal related to the electromagnetic torque (or approximate load) and $x(t)$ is the underlying steady-state stator current to be explored. Combining (3) and (5), we have

$$i_s(t) = h(t) \otimes i_r(t) = h(t) \otimes [m(t)x(t)], \tag{6}$$

where $\otimes$ represents the convolution operation.

Let $y(t)$ denote the measured stator current with additive noise. Therefore, the measured stator current with varying operating conditions can be modeled as

$$y(t) = h(t) \otimes [m(t)x(t)] + n(t), \tag{7}$$

where $n(t)$ represents the measured noise. Equivalently we have the stator current model in frequency domain

$$Y(\omega) = H(\omega)[M(\omega) \otimes X(\omega)] + N(\omega). \tag{8}$$

To rewrite our measurement model in discrete-time (DT) domain, we define $\mathbf{s} = [s[t_0], \; s[t_1], \; \ldots, \; s[t_{N-1}]]^\top$ as a vector of samplings of a time-domain signal $s(t)$ with sampling frequency F_s, where $t \in \{t_n = n/F_s, n = 0, \ldots, N-1\}$. Let $S[f]$ denote the frequency-domain vector of the discrete-time Fourier transform (DTFT) of $\mathbf{s}$, i.e. $S[f] = \mathbf{F}\mathbf{s}$, where $\mathbf{F} \in \mathbb{C}^{N \times N}$ denotes the DTFT operation.

Following the above notation, we use $\mathbf{x}, \mathbf{y}, \mathbf{m}, \mathbf{h}, \mathbf{n} \in \mathbb{C}^N$ to represent the vectors of samplings from $x(t), y(t), m(t), h(t)$, and $n(t)$ respectively. Thus, the time-domain signal model described in (7) can be rewritten as follows:

$$\mathbf{y} = \mathbf{h} \otimes (\mathbf{m} \odot \mathbf{x}) + \mathbf{n}, \tag{9}$$

where $\odot$ represents the element-wise product of two vectors.

2.2. Prior assumptions

Obtaining an estimate of $\mathbf{x}, \mathbf{m}$, and $\mathbf{h}$ from $\mathbf{y}$ amounts to solving a joint blind deconvolution-demodulation problem. This is an ill-posed inverse problem and requires prior knowledge about the nature of $\mathbf{x}, \mathbf{m}$, and $\mathbf{h}$. Based on the physical model of the stator current in the presence of load, the following assumptions about the nature of $\mathbf{x}$, $\mathbf{m}$, and $\mathbf{h}$ are made.

First, we know that $\mathbf{x}$ contains a strong operating frequency signal, its harmonics, and other periodic signals that correspond to the motor fault. In the frequency domain, $\mathbf{x}$ is typically of the form

$$X[f] = \sum_{i=1}^{n_S} A_i \delta[f - f_i], \tag{10}$$

where A_i is the amplitude of frequency component presented at f_i. Therefore, we assume that $\mathbf{F}\mathbf{x}$ is a sparse vector.

Second, we assume that the random load is slowly varying in time. This translates to the assumption that $m(t)$ is band limited with half-bandwidth f_m, *i.e.*,

$$\text{supp}(\mathbf{m}) = [-f_m, f_m]. \tag{11}$$

Lastly, based on the nature of the motor impulse response discussed in Section 2.1, we assume that the form of the magnitude frequency response $h(t)$ is of the form

$$|H[f]| = \mathcal{H}_{\boldsymbol{\alpha},\boldsymbol{\beta}}[f] = \sqrt{\frac{1 + 4\pi\alpha_1\beta_1 f + 4\pi^2\beta_1^2 f^2}{1 + 4\pi\alpha_2\beta_2 f + 4\pi^2\beta_2^2 f^2}}, \tag{12}$$

where $\boldsymbol{\alpha} = [\alpha_1 \;\; \alpha_2]^\top$, $\boldsymbol{\beta} = [\beta_1 \;\; \beta_2]^\top$, related to a, b, c, and d in (3), $\boldsymbol{\alpha}, \boldsymbol{\beta} \in \mathbb{R}^2$, $|\alpha_1|, |\alpha_2| < 1$ (i.e. $\|\boldsymbol{\alpha}\|_\infty < 1$), and the phase $\angle H[f]$ needs to be estimated from the measured data.

3. PROPOSED APPROACH

Based on the prior assumptions described in Sec. 2.2, the problem of MCSA fault detection under varying operating conditions can be cast as the following generalized optimization problem to jointly estimate $\mathbf{h}$, $\mathbf{x}$, and $\mathbf{m}$,

$$\begin{aligned} \{\hat{\mathbf{h}}, \hat{\mathbf{m}}, \hat{\mathbf{x}}\} &= \underset{\{\mathbf{h},\mathbf{m},\mathbf{x}\}}{\arg\min}\, \mathcal{L}(\mathbf{h}, \mathbf{m}, \mathbf{x}) + \lambda_x \psi_x(\mathbf{x}) \\ &= \underset{\{\mathbf{h},\mathbf{m},\mathbf{x}\}}{\arg\min}\, \|\mathbf{y} - \mathbf{h} \otimes (\mathbf{m} \odot \mathbf{x})\|_2^2 + \lambda_x \|\sigma \odot \mathbf{F}\mathbf{x}\|_1 \\ &\quad s.t. \quad \text{supp}(\mathbf{m}) = [-f_m, f_m], \; |H[f]| = \mathcal{H}_{\boldsymbol{\alpha},\boldsymbol{\beta}}[f], \end{aligned} \tag{13}$$

where $\psi_x(\mathbf{x}) = \|\sigma \odot \mathbf{F}\mathbf{x}\|_1$ is a weighted ℓ_1 penalty with weights σ to promote sparsity in $\mathbf{F}\mathbf{x}$. Although a similar optimization problem arises in traditional compressive sensing and blind demodulation, the problem at hand presents significant challenges unique to the physical measurement system. First, the signal $\mathbf{x}$ is affected by both an unknown modulating signal and an unknown filter. Second, $\mathbf{x}$ may contain very weak periodic signatures of the motor fault, which are

typically 40dB to 60dB lower in power than the main operating frequency component at f_s. Moreover, similar to blind deconvolution or demodulation, this is a non-convex optimization problem. Therefore, in order to find a suitable solution, a good initialization of $\mathbf{x}, \mathbf{m}$ and $\mathbf{h}$ is necessary. Our approach to solving this problem is inspired by the proximal alternating linearized minimization (PALM) [15] framework, with careful initialization heuristics and regularization that are described below.

3.1. Initialization heuristics for the optimization variables

In order to make our approach robust to noise, we preprocess the measurements using denoising via minimum-variance (MV) beamforming [11, 12]. Next, since it is known that $\mathbf{x}$ is sparse in the frequency domain and contains the fundamental frequency and harmonics of the operating frequency f_s, we initialize $\mathbf{x}$ as a linear combination of $2n_s$ harmonics of f_s, with the amplitude of each harmonic being equal to the amplitude of that harmonic in the measured data.

$$X_{init}[f] = \sum_{k=-n_s}^{n_s} Y[f] \cdot \delta[f - f_{s,k}], \tag{14}$$

where $f_{s,k}$ is the k^{th} harmonic frequency.

Next, we initialize $\angle H[f] = 0$, and $|H[f]| = \mathcal{H}_{\boldsymbol{\alpha},\boldsymbol{\beta}}[f]$, where $\boldsymbol{\alpha}, \boldsymbol{\beta}$ are to be estimated from the measured data. Considering that $X[f]$ is a sparse weighted sum of delta functions, the forward process in (8) results in $M[f]$ being mirrored onto the peak locations $f_{s,k}$ in the measured data, and further distorted by $H[f]$. Therefore, templates of $M[f]$ can in-principle be obtained from the data by windowing the data around $f_{s,k}$ and correcting for the distortion due to $H[f]$. Since $|H[f]|$ is of the form described in (12), these distortion-corrected templates of $M[f]$ depend upon the choice of $\boldsymbol{\alpha}, \boldsymbol{\beta}$ used to correct for the $H[f]$-distortion. The $H[f]$-distorted template of $M[f]$ at location $f_{s,k}$ can be obtained from the measured data as:

$$\mathcal{M}^{(k)}[f] = \frac{Y[f + f_{s,k}]}{X_{init}[f_{s,k}]} = \frac{Y[f + f_{s,k}]}{Y[f_{s,k}]}, \tag{15}$$

for $|f| < f_b$ according to (11).

Now, for the true value of $\boldsymbol{\alpha}, \boldsymbol{\beta}$, the magnitudes of the distortion-corrected templates $\frac{|\mathcal{M}^{(k)}[f]|}{\mathcal{H}_{\boldsymbol{\alpha},\boldsymbol{\beta}}[f+f_{s,k}]}$ must be close to each other, as well as to the true value of $|M[f]|$. Therefore, the optimal value of $\boldsymbol{\alpha}, \boldsymbol{\beta}$ and the initial estimate of $M[f]$ are computed via the following optimization problem:

$$\begin{aligned}\{\hat{\boldsymbol{\alpha}}, \hat{\boldsymbol{\beta}}, M_{init}\} &= \underset{\boldsymbol{\alpha},\boldsymbol{\beta},M}{\arg\min}\, \mathcal{L}'(\boldsymbol{\alpha}, \boldsymbol{\beta}, M) \\ &= \underset{\boldsymbol{\alpha},\boldsymbol{\beta},M}{\arg\min} \sum_k \varsigma_k^2 \left\| M[f] - \frac{|\mathcal{M}^{(k)}[f]|}{\mathcal{H}_{\boldsymbol{\alpha},\boldsymbol{\beta}}[f + f_{s,k}]} \right\|_2^2,\end{aligned} \tag{16}$$

where ς_k is the signal-to-noise ratio (SNR) at the kth harmonic. We adopt an alternating minimization scheme to solve this problem until convergence. For any feasible value of $\boldsymbol{\alpha}, \boldsymbol{\beta}$, minimizing $\mathcal{L}'(\boldsymbol{\alpha}, \boldsymbol{\beta}, M)$ with respect to M alone is straightforward, and the minimizer is given by

$$\tilde{M}_{\boldsymbol{\alpha},\boldsymbol{\beta}}[f] = \frac{1}{\sum_l \varsigma_l^2} \sum_l \varsigma_l^2 \frac{|\mathcal{M}^{(l)}[f]|}{\mathcal{H}_{\boldsymbol{\alpha},\boldsymbol{\beta}}[f + f_{s,l}]}. \tag{17}$$

Given the solution of M_{init} in (17), the values of $\boldsymbol{\alpha}$ and $\boldsymbol{\beta}$ are then obtained by solving (16) using a blackbox nonlinear least-squares solver. The schematic diagram of estimating $\boldsymbol{\alpha}$, $\boldsymbol{\beta}$, and M_{init} is shown in Fig. 1.

3.2. Modified PALM method for joint blind deconvolution-demodulation

Using the initialization of the optimization variables obtained in Sec. 3.1, the estimates of the variables are obtained via optimization problem (13) representing joint blind deconvolution and demodulation.

Similar problems have been solved using alternating minimization approaches in the context of blind deconvolution [15, 16, 17]. These approaches alternately minimize the objective with respect to $\mathbf{m}$ and $\mathbf{x}$ iteratively. Although simple to describe, it has been shown that the alternating minimization approach is highly sensitive to initialization, and convergence can only be obtained under restrictive conditions. A proximal alternating linearized minimization (PALM) scheme addresses some of these issues by replacing the alternating minimization steps by proximal/projected gradient steps [15]:

$$\mathbf{x}_{k+1} = \text{prox}[(\lambda_x/2)\psi_x](\mathbf{x}_k - \eta_x \nabla_{\mathbf{x}} \mathcal{L}(\mathbf{x}_k, \mathbf{m}_k)), \tag{18}$$

$$\mathbf{m}_{k+1} = \text{proj}_{\{\mathbf{m}|\text{supp}(\mathbf{m})=[-f_m, f_m]\}}(\mathbf{m}_k - \eta_m \nabla_{\mathbf{m}} \mathcal{L}(\mathbf{x}_{k+1}, \mathbf{m}_k)), \tag{19}$$

where for a function $\psi : \mathbb{C}^N \to \mathbb{R}$ and $\mathbf{v} \in \mathbb{C}^N$, the proximal operator is defined as

$$\text{prox}[\psi](\mathbf{v}) = \underset{\mathbf{w}}{\arg\min}\, \psi(\mathbf{w}) + \frac{1}{2} \|\mathbf{v} - \mathbf{w}\|_2^2, \tag{20}$$

and for a set $\mathcal{S}$, $\text{proj}_{\mathcal{S}}(\mathbf{v})$ is the projection of $\mathbf{v}$ onto $\mathcal{S}$. In our approach, the proximal-gradient steps for $\mathbf{x}$ and $\mathbf{m}$ are interspersed with updates to $\mathbf{h}$. Also, from (7), it is clear that once $\hat{\mathbf{x}}$ is recovered, the stator current without varying load can be obtained by

$$\hat{\mathbf{s}} = \hat{\mathbf{h}} \otimes \hat{\mathbf{x}}, \tag{21}$$

where $\hat{\mathbf{h}}$ and $\hat{\mathbf{x}}$ are outputs of the optimization problem defined in (13). The entire proposed procedure is summarized in Alg. 1.

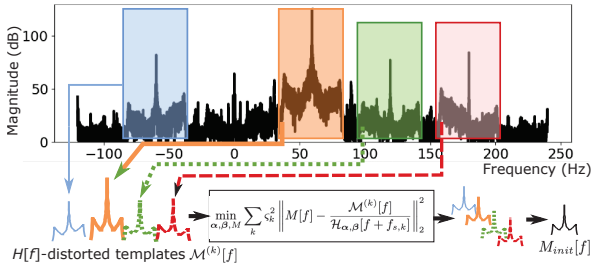

Fig. 1. Schematic diagram for estimating $\boldsymbol{\alpha}, \boldsymbol{\beta}$ and M_{init}. As described in Sec. 3.1, templates of $M[f]$ distorted by $H[f]$ are first extracted from the measured data. They are fed into the optimization problem (16) which finds $\boldsymbol{\alpha}, \boldsymbol{\beta}$ such that the weighted variance between the distortion-corrected templates $\mathcal{M}^{(k)}[f]/\mathcal{H}_{\boldsymbol{\alpha},\boldsymbol{\beta}}[f+f_{s,k}]$ is minimized.

4. EXPERIMENTAL RESULTS

To examine our approach, we consider stator current data collected from a motor with eccentricity fault. The motor is operating at

Algorithm 1 Proposed algorithm for blind signal recovery

Input : $\mathbf{y} \leftarrow \mathbf{y}_{\text{bf}}$ (MV beamformed measurements)
Set $k = 0$ and initialize $\mathbf{x}_0 = \mathbf{F}^{-1}(X_{init}[f])$ according to (14).
Compute $\hat{\boldsymbol{\alpha}}$, and $\hat{\boldsymbol{\beta}}$, initialize $\mathbf{m}_0 = \mathbf{m}_{init} = \mathbf{F}^{-1}(\tilde{M}_{\hat{\boldsymbol{\alpha}},\hat{\boldsymbol{\beta}}}[f])$, as described in Section 3.1.
while $\mathbf{x}_k$ is not converged **do**
  $\angle H_{k+1}[f] \leftarrow \angle \frac{Y[f](M_k \otimes X_k)^*[f]}{\mathcal{H}_{\boldsymbol{\alpha},\boldsymbol{\beta}}[f]|(M_k \otimes X_k)[f]|^2 + \epsilon}$, $|H_{k+1}| = H_{\boldsymbol{\alpha},\boldsymbol{\beta}}$
  $\mathbf{h}_{k+1} = \mathbf{F}^{-1}(H_{k+1}[f])$
  $\mathbf{x}_k \leftarrow \mathbf{x}_k - \eta_x \nabla_{\mathbf{x}_k} \|\mathbf{y} - \mathbf{h}_{k+1} \otimes (\mathbf{m}_k \odot \mathbf{x}_k)\|_2^2$
  $\mathbf{x}_{k+1} \leftarrow \text{prox}[\lambda_x \|\sigma \odot \mathbf{F}\mathbf{x}_k\|_1](\mathbf{x}_k)$
  $\mathbf{m}_{k+1} \leftarrow \mathbf{m}_k - \eta_m \nabla_{\mathbf{m}_k} \|\mathbf{y} - \mathbf{h}_{k+1} \otimes (\mathbf{m}_k \odot \mathbf{x}_{k+1})\|_2^2$
  $k \leftarrow k + 1$
end while
Output : $\hat{\mathbf{s}} = \mathbf{h}_k \otimes \mathbf{x}_k$.

$f_s = 60$Hz with either a periodically varying load or a randomly varying load. In the case of the periodically varying load, two variation patterns are considered: a sinusoidal and a rectangular variations with a frequency of 2Hz. In our approach, we set the half-bandwidth of $\mathbf{m}$ to be $f_m = 26$Hz. The sparsity weight $\sigma[f]$ is set to $e^{-\varepsilon[f]}$, where $\varepsilon[f]$ is the smooth envelope of $\log|Y[f]|$ computed using the procedure described in [18]. The signal-to-noise ratio (SNR) at peak location $f_{s,k}$ is computed as $\varsigma_k = |Y[f_{s,k}]|/\eta$, with η being the average noise level in a 1 Hz window on either side of the template support $[f_{s,k} - f_m, f_{s,k} + f_m]$. We compare our approach to the MV-beamforming method [11, 12], which is effective at reducing the noise in the measured current signal, but unable to remove structured artifacts due to the varying load.

4.1. Stator current with periodically modulated load

Figures 2(a) shows the time-domain stator signal for the sinusoidally and rectangularly modulated load respectively, each with measured data and processed data. It can be seen that for both cases, the proposed approach significantly reduced the impact of modulation due to the varying load. Since only the dominant $f_s = 60$Hz mode can be clearly observed in the time-domain, we further compare the frequency-domain signals for details.

Figures 2(b) and 2(c) show the frequency domain stator signal for the sinusoidally and rectangularly modulated load respectively, along with the stator signal recovered using the MV beamforming approach, and the proposed approach. These plots show that as expected, MV beamforming is successful in denoising the signal, because it effectively destroys the noise by averaging over the random phase components of the noise, while adding structured periodic signal sections constructively. However, MV beamforming is unable to remove the artifacts due to load variation, since these artifacts are structured. It can be seen that the proposed approach is effective in removing the effects of load variation. The eccentricity fault signatures can be clearly seen around 30Hz and 90Hz while the corresponding rotor frequency $f_r = 30$Hz, which agrees with the MSCA-based fault detection model.

4.2. Stator current with randomly modulated load

Next, signal recovery in the case of the more realistic scenario of randomly varying load was examined. The time- and frequency-domain representations of the measured and the recovered signals can be seen in Fig. 3 and Fig. 4 respectively. From the time-domain plot, it can be seen that the impacts of modulation are reduced by the proposed algorithm. In the frequency-domain plot, it can be seen

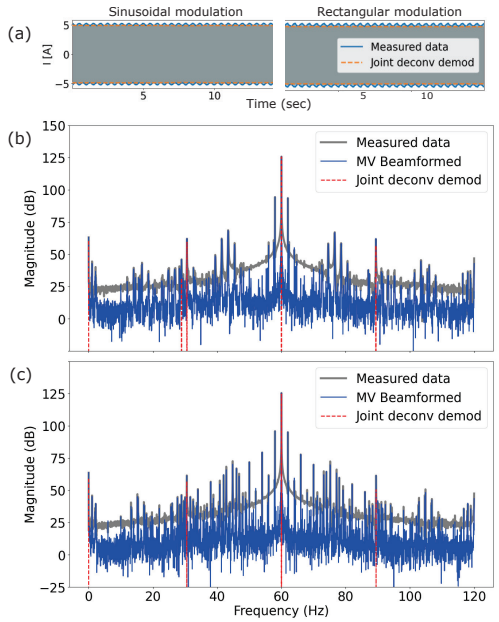

Fig. 2. (a) The blue and the orange curves represent measured and recovered stator signals in the time domain for sinusoidal and rectangular load modulation, respectively. (b) & (c) Measured and recovered stator signals in the frequency domain for sinusoidal and rectangular load modulation respectively.

that the proposed approach is effective in reducing the noise as well as the effects of the random convolution and modulation, and is able to retain the eccentricity fault signatures at around 30Hz and 90Hz respectively.

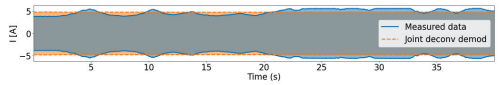

Fig. 3. Measured and recovered stator currents in the time domain for random load

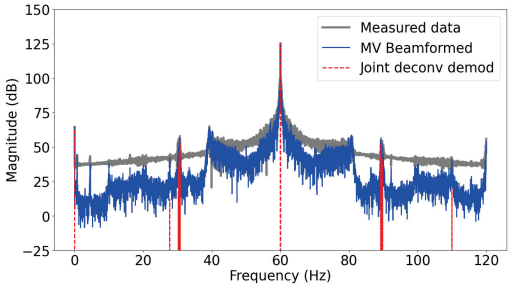

Fig. 4. Measured and recovered stator currents in the frequency domain for random load

5. CONCLUSION

In this work, we proposed an approach for sparsity-driven joint blind demodulation and deconvolution of stator signals containing eccentricity fault signatures. We showed that our approach successfully suppress noise and remove the unknown modulating effects of a randomly varying load. Since our approach does not depend specifically upon an assumed model of the types of faults, it can be extended to detecting other types of faults in a motor. Future work could also involve a detection task-based assessment of the proposed algorithm.

6. REFERENCES

[1] S. Nandi, S. Ahmed, and H.A. Toliyat, "Detection of rotor slot and other eccentricity related harmonics in a three phase induction motor with different rotor cages," *IEEE Transactions on Energy Conversion*, vol. 16, no. 3, pp. 253–260, 2001.

[2] M El Hachemi Benbouzid, "A review of induction motors signature analysis as a medium for faults detection," *IEEE transactions on industrial electronics*, vol. 47, no. 5, pp. 984–993, 2000.

[3] Subhasis Nandi, Hamid A Toliyat, and Xiaodong Li, "Condition monitoring and fault diagnosis of electrical motors—a review," *IEEE transactions on energy conversion*, vol. 20, no. 4, pp. 719–729, 2005.

[4] Shahin Hedayati Kia, Humberto Henao, and Gérard-André Capolino, "Efficient digital signal processing techniques for induction machines fault diagnosis," in *2013 IEEE Workshop on Electrical Machines Design, Control and Diagnosis (WEMDCD)*. IEEE, 2013, pp. 232–246.

[5] Jawad Faiz and SMM Moosavi, "Eccentricity fault detection–from induction machines to DFIG—a review," *Renewable and Sustainable Energy Reviews*, vol. 55, pp. 169–179, 2016.

[6] Lucia Frosini, "Novel diagnostic techniques for rotating electrical machines—a review," *Energies*, vol. 13, no. 19, pp. 5066, 2020.

[7] Genyi Luo, JED Hurwitz, and Thomas G Habetler, "A survey of multi-sensor systems for online fault detection of electric machines," in *2019 IEEE 12th International Symposium on Diagnostics for Electrical Machines, Power Electronics and Drives (SDEMPED)*. IEEE, 2019, pp. 338–343.

[8] Martin Blodt, Marie Chabert, Jrmi Regnier, and Jean Faucher, "Mechanical load fault detection in induction motors by stator current time-frequency analysis," *IEEE Transactions on Industry Applications*, vol. 42, no. 6, pp. 1454–1463, 2006.

[9] N Yassa, M Rachek, and H Houassine, "Motor current signature analysis for the air gap eccentricity detection in the squirrel cage induction machines," *Energy Procedia*, vol. 162, pp. 251–262, 2019.

[10] Francisco Vedreño-Santos, Martin Riera-Guasp, Humberto Henao, M Pineda-Sénchez, and Jose A Antonino-Daviu, "Diagnosis of eccentricity in induction machines working under fluctuating load conditions, through the instantaneous frequency," in *IECON 2012-38th Annual Conference on IEEE Industrial Electronics Society*. IEEE, 2012, pp. 5108–5113.

[11] Dehong Liu, Hiroshi Inoue, and Makoto Kanemaru, "Robust motor current signature analysis (mcsa)-based fault detection under varying operating conditions," in *2022 25th International Conference on Electrical Machines and Systems (ICEMS)*. IEEE, 2022.

[12] Robert G Lorenz and Stephen P Boyd, "Robust minimum variance beamforming," *IEEE transactions on signal processing*, vol. 53, no. 5, pp. 1684–1696, 2005.

[13] Peter Vas, *Electrical machines and drives: a space-vector theory approach*, vol. 1, Clarendon press Oxford, 1992.

[14] Bahram Amin, *Induction motors: analysis and torque control*, Springer Science & Business Media, 2001.

[15] Jérôme Bolte, Shoham Sabach, and Marc Teboulle, "Proximal alternating linearized minimization for nonconvex and nonsmooth problems," *Mathematical Programming*, vol. 146, no. 1, pp. 459–494, 2014.

[16] Willard I Zangwill, *Nonlinear programming: a unified approach*, vol. 52, Prentice-Hall Englewood Cliffs, NJ, 1969.

[17] Michael JD Powell, "On search directions for minimization algorithms," *Mathematical programming*, vol. 4, no. 1, pp. 193–201, 1973.

[18] Mantas Gabrielaitis, "Fast and accurate amplitude demodulation of wideband signals," *IEEE Transactions on Signal Processing*, vol. 69, pp. 4039–4054, 2021.